AD A094030

LEVEL

(1)

ESTABLISHMENT OF ENGINEERING DESIGN DATA FOR
HYBRID STEEL/CERAMIC BALL BEARINGS

Phase II

F. R. MORRISON
T. YONUSHONIS

DTIC

JAN 23 1981

C

SEPTEMBER 26, 1980

Final Report on Contract Number N00019-79-C-0418

Approved for public release: distribution unlimited

Prepared for:
U. S. DEPARTMENT OF THE NAVY
NAVAL AIR SYSTEMS COMMAND
CODE - AIR 5163D4
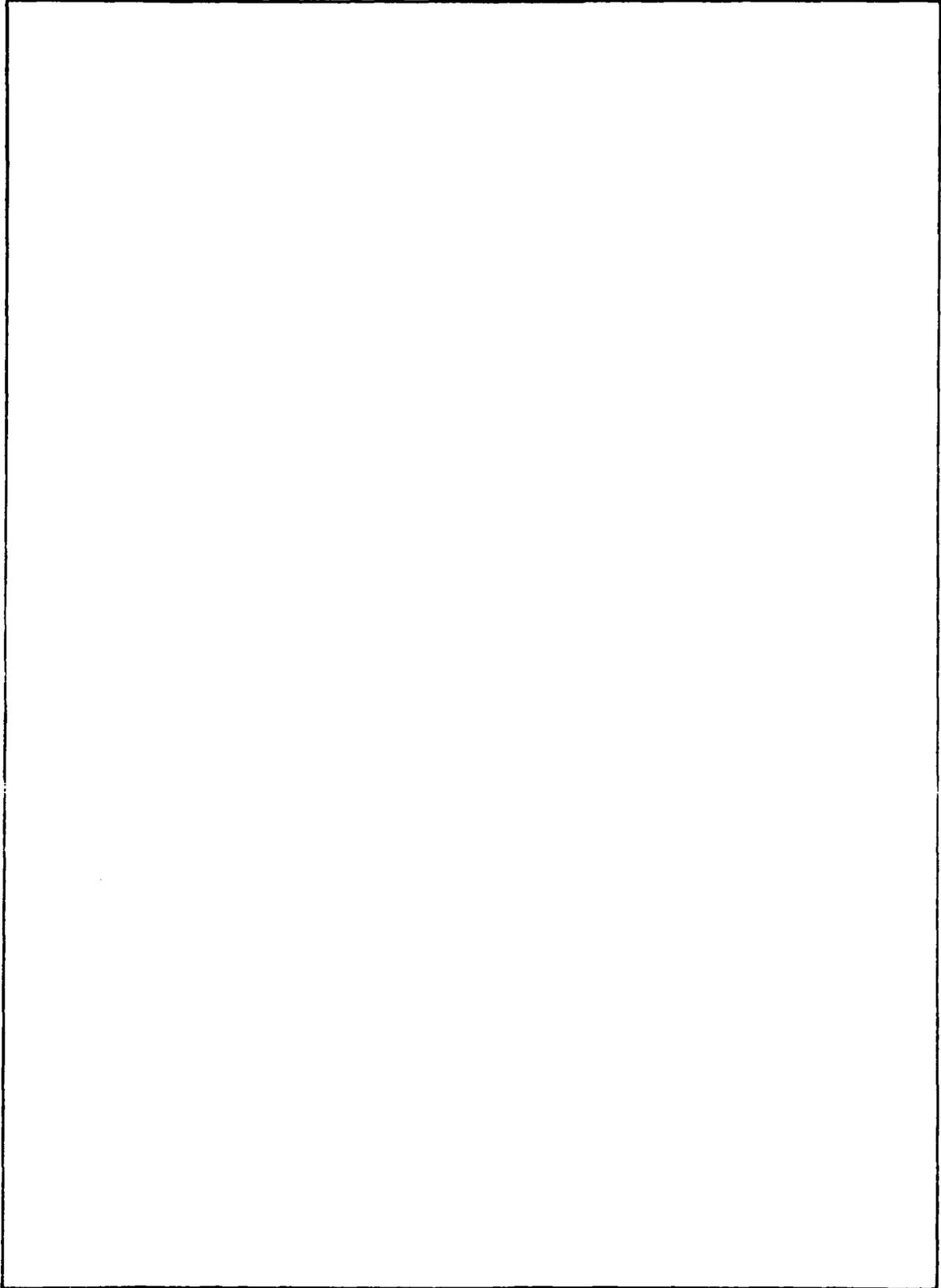WASHINGTON, D. C. 20361

SKF TECHNOLOGY SERVICES

80 0 21 051

SECURITY CLASSIFICATION OF THIS PAGE *(When Data Entered)*

REPORT DOCUMENTATION PAGE		READ INSTRUCTIONS BEFORE COMPLETING FORM
1. REPORT NUMBER	2. GOVT ACCESSION NO. $AD-A094030$	3. RECIPIENT'S CATALOG NUMBER
4. TITLE *(and Subtitle)* Establishment of Engineering Design Data for Hybrid Steel/Ceramic Ball Bearings - Phase II (14) SKF		5. TYPE OF REPORT & PERIOD COVERED Final Report, August 1979-August 1980
		6. PERFORMING ORG. REPORT NUMBER -AT80T042
7. AUTHOR(s) F. R. Morrison, T. Yonushonis		8. CONTRACT OR GRANT NUMBER(s) N00019-79-C-0418
9. PERFORMING ORGANIZATION NAME AND ADDRESS SKF Technology Services 1100 First Avenue King of Prussia, Pa. 19406		10. PROGRAM ELEMENT, PROJECT, TASK AREA & WORK UNIT NUMBERS
11. CONTROLLING OFFICE NAME AND ADDRESS Naval Air Systems Command Code AIR-5163D4 Washington, D. C. 20361		12. REPORT DATE September 26, 1980
		13. NUMBER OF PAGES 57
14. MONITORING AGENCY NAME & ADDRESS*(if different from Controlling Office)* DCASMA, Philadelphia P. O. Box 7699 Philadelphia, Pennsylvania 19101		15. SECURITY CLASS. *(of this report)* UNCLASSIFED
		15a. DECLASSIFICATION/DOWNGRADING SCHEDULE

16. DISTRIBUTION STATEMENT *(of this Report)*

Approved for Public Release: Distribution Unlimited

17. DISTRIBUTION STATEMENT *(of the abstract entered in Block 20, if different from Report)*

18. SUPPLEMENTARY NOTES

19. KEY WORDS *(Continue on reverse side if necessary and identify by block number)*

Silicon Nitride, Rolling Contact Bearings, Hybrid Ball Bearings, Fatigue Life

20. ABSTRACT *(Continue on reverse side if necessary and identify by block number)*

A lot of hybrid ceramic/steel angular contact ball bearings was fabricated to a design optimized for operation at 2.5 x 10⁶ dN. Life tests were conducted on these bearings at low speed, 0.4 x 10⁶ dN, using two load levels which produced maximum Hertz stress levels of 2.0 GPa and 2.4 GPa respectively. A detailed failure analysis was completed to define the causes of the relatively early ball failures experienced at the high load and verify the good performance achieved at the low load.

DD $_{1 \text{ JAN } 73}^{\text{FORM}}$ **1473** EDITION OF 1 NOV 65 IS OBSOLETE

TABLE OF CONTENTS

Page Number

i

1. INTRODUCTION

This report presents the results of an experimental study conducted by SKF Technology Services, a division of SKF Industries, Inc. located in King of **Prussia**, Pa. for the U. S. **Naval** Air Systems Command, Washington, D. C. 20361 under contract N00019-79-C-0418. This is the final technical report issued on this program which was conducted during the period extending from August, 1979 to August, 1980.

1.1 Background

Typically, the operating efficiency of a gas turbine engine is directly related to the rotational speed of the shaft and the temperature attainable in the combustion chamber. Material properties and system operating characteristics produce practical limitations on the allowable levels of these parameters, and thus limit power unit efficiency.

The rolling contact bearings which are used to support the turbine shaft have been one area where limits have been experienced. Bearing steels and lubricants have finite high temperature limits which must be respected if acceptable bearing performance and life are to be achieved. Furthermore, the increased centrifugal forces experienced at high speeds produce loads on the outer ring which can produce significant reductions in bearing life. To date, advances in bearing technology have kept pace with turbine development so that the bearings have not been a key limiting factor. However, if this trend is to continue, it would appear that novel approaches will be required to overcome the bearing design limitations.

One new approach considered as a solution to these problems is the use of ceramic bearing materials. A prime candidate for this application is hot pressed silicon nitride which is characterized by low mass, a resistance to extreme temperatures, a low coefficient of sliding friction, and high wear resistance. A significant amount of effort has been expended during the past decade to show that hot pressed silicon nitride is suitable for use as a bearing material [1-3*], developing finishing techniques which will provide surface textures acceptable for rolling bearing operation on ceramic components [4-8], evaluating the performance characteristics of hybrid steel/ceramic bearings [9-11], and accumulating life data on ceramic components [12-14]. The results of these programs have been positive and effort is now underway to develop the manufacturing technology to fabricate all ceramic bearings [15].

*Numbers in brackets refer to references listed in Section 10

1

To take full advantage of the improved performance potential of ceramic bearings, it is necessary to design systems specifically for this purpose. However, significant performance improvements can be achieved in current systems without experiencing the cost impact of system redesign by using hybrid bearing assemblies comprised of steel rings and ceramic rolling elements. The feasibility of using hybrid bearings had been demonstrated in a number of experimental programs [10, 11, 13]. However, before these bearings could be used in practical systems, basic design data was needed to allow designers to select the specific bearing sizes and configurations which would yield acceptable life and performance in their applications. Specifically, data was required to define the optimization of internal bearing geometries to capatalize on the lower density and increased hardness of the ceramic material; to establish the load-life relationship so that valid life predictions could be calculated; and to establish the effects of variations in lubricant flow rate on bearing performance.

The angular contact ball bearings used to support the shaft of an aircraft gas turbine engine are subjected to high speed, high temperature, and moderate loads. Since this is the primary application considered for a hybrid steel/ceramic bearing, it would be desirable to compile test data under these conditions. However, an endurance test sequence sufficient to establish a load-life relationship is quite extensive. The accumulation of this large amount of data in a reasonable time frame requires the use of high loads to limit individual test duration and multiple test machines to limit the total calendar time. These practical considerations require the basic life data be accumulated on standard endurance test machines which run at moderate speeds and temperatures.

The procedures necessary to extrapolate these test results to gas turbine conditions are well established for steel rolling bearings. It is, however, uncertain that these are equally applicable to steel/ceramic hybrid bearings. Thus, it is necessary to obtain experimental data at high speed, high temperature conditions to verify the validity of the extrapolation.

A multi-phase program planned to accumulate the described data was initiated in April, 1978. However, the validity of the initial life test data was compromised by the use of an experimental ceramic processing technique called "near net shape processing" [16]. The current program sponsored by the U. S. Naval Air Systems Command under Contract Number N00019-79-C-0418 is a reinitiation of that effort which uses ceramic material processed in billet form and established machining and finishing techniques. The results achieved in this program are described in this report.

2

1.2 Technical Objectives

Conventionally, a system designer will calculate the life of a rolling contact bearing using load-life formulations developed by Lundberg and Palmgren [17, 18]. These formulae define the rating life of a lot of bearings, i.e. the life that 90% of the bearings will meet or exceed, as follows;

$$L_{10} = (C/P)^p$$

where:

L_{10} = Bearing rating life in millions of revolutions;

C = Basic bearing load rating in pounds (Bearing Catalog Value);

P = Equivalent bearing load, lbs; and

p = Life exponent: 3 for ball bearings and 10/3 for roller bearings

Recently technological advances in bearing design, steel processing, and manufacturing techniques have resulted in potential improvements in bearing life expectancy. Furthermore, it is also now possible to account for the effects of application conditions on bearing life. To include these effects, a new life formula has been introduced [19]. That is;

$$L'_n = a_1 \, a_2 \, a_3 \, L_{10}$$

where:

L'_n = The adjusted, expected theoretical bearing life;

a_1 = Life adjustment factor for reliability (90%=1);

a_2 = Life adjustment factor for material; and

a_3 = Life adjustment factor for application conditions, such as film thickness

The use of the life adjustment factors allows the systems designer to directly estimate bearing life according to the needs and operating characteristics of his specific application.

The overall objective of this experimental effort is to accumulate sufficient life data on ceramic/steel hybrid bearings to define preliminary values for the life adjustment factors as well as the basic life formulation. Specifically, values for the exponent of the load-life relationship, p , and the material life adjustment factors, a_2a_3, will be developed. While the final-ization of these values will require the accumulation of a large quantity of statistical data, the availability of the preliminary values will provide a basis for design engineers to incorporate hybrid bearings into new and currently operating systems.

4

2. TEST BEARING DESIGN

The material properties of silicon nitride are significantly different from those of steel. The conventional bearing designs which optimize the life and performance of steel bearings are not optimum for ceramic/steel hybrid bearings. A detailed bearing design analysis was conducted as part of the previous program [16] to optimize the geometry of a hybrid bearing for a hypothetical aircraft gas turbine engine. It was planned to run the bulk of the life tests at a relatively low speed, i.e. 1016 rad/s (9700 rpm) where centrifugal effects are minimal. The number of balls in the bearing was reduced from the normal complement of 14 to 7 to provide economical test specimens. The same bearing design, designated 7209 VAN, was also used for the low speed endurance tests of the current program. This bearing is illustrated in Figure 1.

Both steel and hybrid bearings were also required for the 2.5×10^6 dN performance and life tests. At these high speeds, i.e. 5760 rad/s (55,000 rpm), centrifugal effects are significant and the reduced ball complement could have an adverse affect on overall bearing performance. The bearings to be used in these tests were therefore specified to have the normal number of rolling elements. These bearings were fabricated using ring designs identical to those of the 7209 VAN and fourteen balls of either silicon nitride or steel. These latter bearing designs were designated as 7209 VAR and 7209 VAS and are illustrated in Figures 2 and 3.

5

Figure 1

ABEC 5 TOLERANCES
N° OF BALLS – 7
BALL DIA. (DW) – 12.7mm (0.50")
GROOVE CURVATURE:
INNER RACEWAY – 51%
OUTER RACEWAY – 52%

| C = | 18800 N | = | 4200 LBS |
| C_o = | 11700 N | = | 2625 LBS |

e	$\frac{F_a}{F_r} \le e$		$\frac{F_a}{F_r} > e$		Y_o
	X	Y	X	Y	
.86	1	0	.38	.71	.62
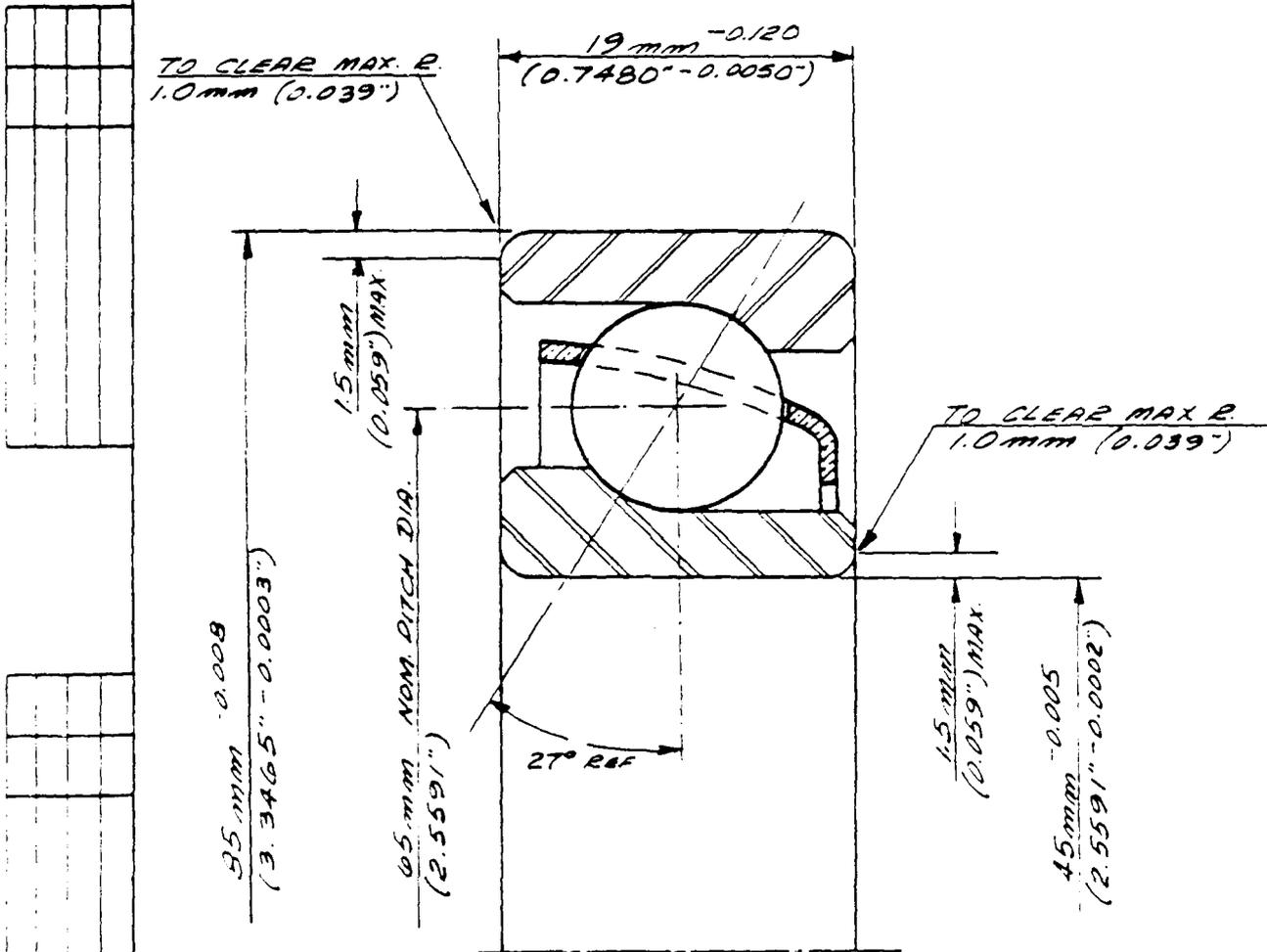
TO CLEAR MAX. R.
1.0mm (0.039")

19mm −0.120
(0.7480" − 0.0050")

1.5mm
(0.059") MAX.

35 mm −0.008
(3.3465" − 0.0003")

Ø65 mm NOM. PITCH DIA.
(2.5591")

27° REF

TO CLEAR MAX R.
1.0mm (0.039")

1.5 mm
(0.059") MAX.

45mm −0.005
(2.5591" − 0.0002")

MATERIALS:
INNER & OUTER RINGS – VIMVAR M50
BALLS – NC132 Si_3N_4
CAGE – PRESSED BRASS

CUSTOMER : NAVAIR

EDITION / YEAR-MO	1	2	3	4	5	6

SKF   SKF INDUSTRIES, INC

DRAWN	CHECK	APPR	REG
B	J.H	X	DATE 10 2 79

SCALE

SINGLE ANGULAR
CONTACT BALL BEARING

BEARING NO:

7209 VAN

Figure 2

ABEC 5 TOLERANCES
No OF BALLS - 14
BALL DIA. (Dw) - 12.7mm (0.50")
GROOVE CURVATURE:
 INNER RACEWAY - 51%
 OUTER RACEWAY - 52%

	27,500 N	6,200
	21,200 N	4,750

e	$\dfrac{F_a}{F_r} \le e$		$\dfrac{F_a}{F_r} > e$	
	X	Y	X	Y

TO CLEAR MAX. R.
_1.0 mm (0.039")_

19 mm -0.120
(0.7480" -0.0050")

15 mm
(0.059") MAX.

85 mm -0.008
(3.3465" -0.0003")

65 mm NOM. PITCH DIA.
(2.5591")

27° REF.

TO CLEAR MAX. R.
_1.0 mm (0.039")_

15 mm
(0.059") MAX.

45 mm -0.005
(2.5591" -0.0002")

MATERIALS:
INNER & OUTER RINGS - VIMVAR M50
BALLS - NC 132 Si$_3$N$_4$
CAGE - PRESSED BRASS

CUSTOMER: NAVAIR

	YEAR-NO	1	2	3	4	5	6
					DRAWN	CHECK	APPR	REG REIPP

SKF

SKF INDUSTRIES, INC

DRAWN KARMAN
DATE SEPT. 18, 1980

SINGLE ANGULAR
CONTACT BALL BEARING

BEARING NO
7209 VAR

ABEC 5 TOLERANCES
NO OF BALLS - 14
BALL DIA. (Dw) - 12.7 mm (0.50")
GROOVE CURVATURE:
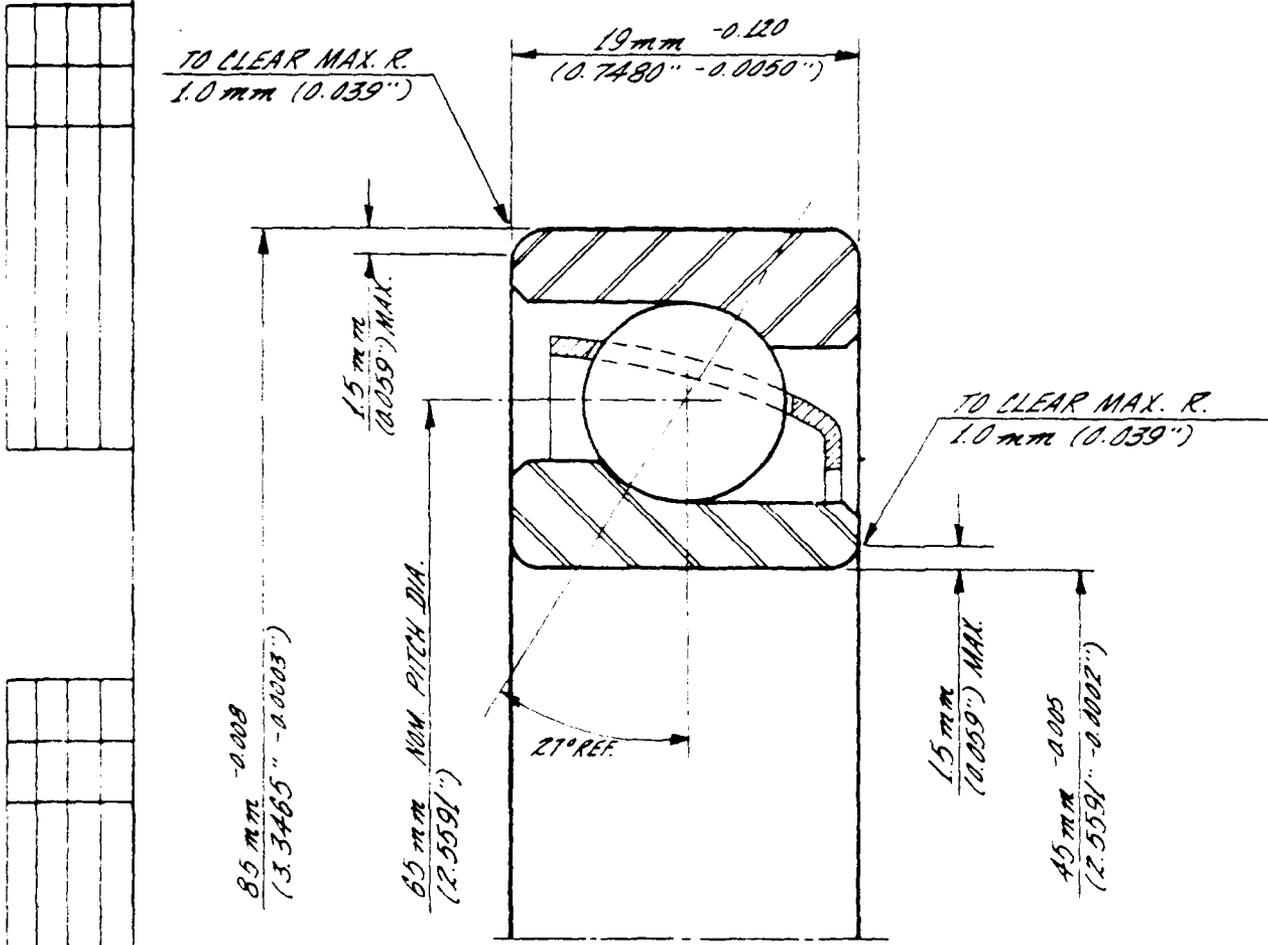 INNER RACEWAY - 51%
  OUTER RACEWAY - 52%

22,500 N   5,200
21,200 N   4,750

19 mm $^{-0.120}$
(0.7480" -0.0050")

TO CLEAR MAX. R.
10 mm (0.039")

15 mm (0.059") MAX.

TO CLEAR MAX R.
10 mm (0.039")

85 mm NOM. PITCH DIA.
(2.559")

27° REF.

15 mm (0.059") MAX.

45 mm -0.005
(2.5521" -0.0002")

MATERIALS:
INNER & OUTER RINGS - VIMVAR M50
BALLS - VIMVAR M50
CAGE - PRESSED BRASS

SKF INDUSTRIES, INC
DRAWN
DESIGN
APPD
REG
DATE SEPT 18 1980

NO	1	2	3	4	5	6

SINGLE ANGULAR
CONTACT BALL BEARING

BEARING NO.
7209 VAS

3. TEST BEARING PREPARATION

A total of eighty-four angular contact ball bearings were manufactured for use in this experimental program. Sixty bearings are of the 7209 VAN hybrid design having one half the normal ball complement; twelve are 7209 VAR hybrid bearings having a full complement of balls; and the remaining twelve are all steel 7209 VAS bearings with fourteen steel balls. The experimental nature of the bearing design and the use of material not currently used in bearing manufacturing precluded the use of standard production facilities for this effort. The manufacturing activities were primarily completed within the facilities maintained by SKF Technology Services. A description of the fabrication processes is contained in the following paragraphs.

3.1 Steel Components

The inner and outer rings were machined from bar stock of vacuum induction melted, vacuum arc remelted (VimVar) M50 tool steel, a standard aircraft bearing material. The raw material had been source inspected and certified using standard procedures for the acceptance of material for use in bearings for aircraft applications. The machined parts were heat treated to produce a minimum hardness of $R_c 60$, by an approved SKF subcontractor certified for the processing of components for aircraft bearings. The hardened components were rough ground on all critical surfaces to eliminate heat treat distortions. This was followed by stress relieving and finish grind operations on all specified ground surfaces.

Dimensional control of the finished parts was maintained through a two stage process of set-up control. Initial set-up pieces were measured using shop working gauges, preset for a specific parameter to standards traceable to the National Bureau of Standards. When shop standards indicated that the set-up was acceptable, a part was submitted to the Metrology Laboratory for verification of acceptability and documentation. The test lot was subsequently processed using the verified set-up.

Final inspection of the components included 100% magnetic particle inspection, 100% nital etch, and 100% visual examination of the critical groove contact surfaces, employing existing acceptance procedures for aircraft bearing components. The evidence of the etch inspection was removed by polishing, as is the standard practice, to highlight any discontinuities on the contact surfaces, eg. nicks, dents, grinding furrows, and to facilitate the inspection of these rings by visual means.

A dimensional audit was conducted on a five bearing sample to insure that the described in-process controls had been satisfactory to control finished part geometry. Measurements were made of (1) inner and outer ring cross groove radius, (2) inner and outer ring cross groove profile, (3) inner and outer ring cross groove surface roughness, and (4) assembled bearing contact angle. This audit sequence established that the dimensional quality of the bearings was acceptable for the conduct of a life test program.

The M50 tool steel balls were obtained from a stock lot specifically manufactured for use in bearings for aircraft applications. Since these components had previously been subjected to the material qualification and dimensional control audits specified for these critical bearings, the balls were used as received.

3.2 Silicon Nitride Components

3.2.1 Introduction

The ceramic material used for the manufacture of the 12.7 mm (0.500 inch) diameter balls was Noralide NC132 hot pressed silicon nitride obtained from Norton Company. Quality control measures were implemented in the areas of raw material inspection and non-destructive evaluation to assure production of the highest quality silicon nitride balls. Hot pressed silicon nitride was obtained in billet form in order to avoid density variations and inclusions associated with near-net shape hot pressing of silicon nitride powders [16]. The effectiveness of the quality control procedures and the use of billet material resulted in uniform ball density, and minimal reject rate observed during fluorescent dye penetrant inspection of the finished components.

3.2.2 Norton Certification

The Norton certification data of powder lot HN-15 and the billets used in this program are presented in Appendix A. Quality control procedures at Norton consist of analyzing the powder lot for key elements, and checking the individual billets for flexure strength at room temperature and 1643 K (2500°F), structural consistancy using x-ray radiographic techniques, and density. In addition to these measurements, proprietary processing parameters are monitored and analyzed by Norton. All billets used in this program exceeded the minimum requirements for Noralide NC132 hot pressed silicon nitride (HPSN).

10

3.2.3 SKF Material Certification

SKF Technology Services augmented the Norton quality control procedures with additional x-ray radiographic inspection, fracture surface analysis, optical analysis, density and hardness measurements. These additional evaluations provided the maximum amount of information on billet quality with a minimum cost and schedule impact.

3.2.3.1 X-ray Radiography: A 150 mm x 15 mm x 3 mm slice was cut from each HPSN billet received from Norton. These sections were x-ray radiographed to check for possible segregation or x-ray density variations in planes parallel to the hot pressing direction. Figure 4 shows a photographic print of the HPSN cross sections made by using the microfocus x-ray radiograph as a negative. Billet 1283 had significant x-ray density variations. Although the cause of x-ray density variations has not been identified and the effect of x-ray density variations on rolling contact fatigue performance are unknown, Norton Company replaced this billet.

3.2.3.2 Fracture Surface and Ceramographic Analysis: Using samples taken from each billet, fracture surfaces were analyzed by scanning electron microscopy and polished sections were analyzed optically by Nomarskii interference contrast. Figure 5 shows typical SEM micrographs of fracture surfaces and optical micrographs of the silicon nitride microstructure. HPSN fracture surfaces were analyzed using the scanning electron microscope in the secondary electron and backscattered electron imaging modes. Fracture surfaces from billet to billet were for all practical purposes identical. Both intergranular and transgranular fracture were observed which is typical of HPSN. Microscopic analysis of the polished sections was unable to distinguish differences in inclusion content from billet to billet. However, low power and visual observations had revealed slight differences in the material's polishing behavior. In the extreme, variations of this nature could produce differences in the surface characteristics of the finished parts. However, the differences noted in this instance were not thought to be significant.

In general, these evaluations demonstrated that the ceramic material was fine grained, dense and uniform in structure. While, low power optical analysis indicated subtle billet to billet variations, SEM and optical microscopic confirmed that the silicon nitride material was acceptable for processing.

Figure 4.

Billet
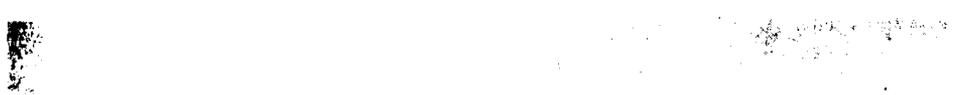Number

1280

1281

1282

1283

1284

1285

1292

1293

1294

1295

1296

1297

Figure 5. Photomicrographs of Silicon Carbide ... are ... ...

Billet ...   ...   Billet x

A. Typical polished section. Nomarski interference ... ...ist
   Black ... ... are pullouts, gray ... ...he
   white ... ... contaming phases

Billet 500x
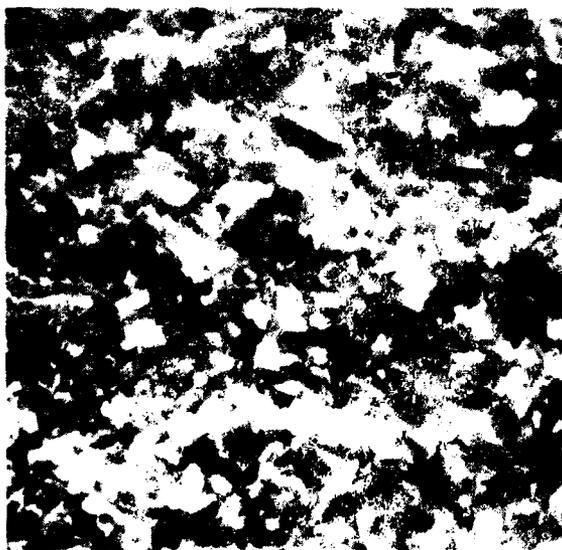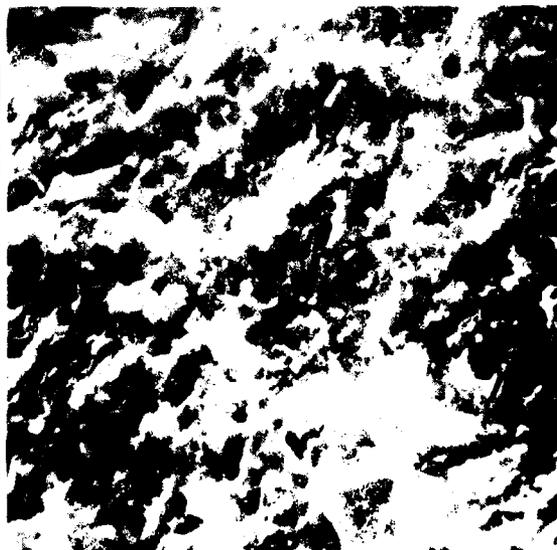
3.2.3.3 Hardness and Density: Vicker's, diamond pyramid, hardness was measured under a 500 gram load on the polished sections. These data, presented in Table 1, show slight differences in hardness from billet to billet, but these variations were not significant. All of the hardness values greatly exceeded the minimum value of 1400 kg/mm^2 specified for silicon nitride material by SKF.

The density of thirty-four finished balls selected at random was calculated using measured ball dimensions and dry weight. These data are given in Table 2. The average density of the balls was 3.25 g/cm^3 which was in good agreement with Norton's certification data. The measured density of each ball exceeds SKF's minimum requirement of 3.2 g/cm^3. This is a positive result since it can be recalled that 13% of the near-net shape hot pressed silicon nitride balls which demonstrated poor endurance lives in the previous program [16] had densities below 3.2 g/cm^3.

3.2.4 Grinding, Lapping, and Polishing Silicon Nitride

Norton certified and SKF approved NC132 HPSN billets were forwarded to Bullen Ultrasonics for rough grinding operations. The silicon nitride billets were ultrasonically ground into rough spheres having a 13 mm (0.512 in.) diameter, i.e. 0.3 mm (0.012 in.) larger than the finished ball size. Surface roughness of the ultrasonically ground spheres was excellent, 0.08 to 0.16 um AA (3 to 6 µ in. AA) and two point out of roundness was limited to 1 to 5 µm (40 to 200 µ in.).

Ultrasonically ground balls were further processed using the ball finishing facility at SKF Technology Services. The balls were visually inspected, then lapped with 500 grit SiC abrasive in a multigroove lapping machine to improve ball roundness and surface finish. Approximately 0.03 mm (0.012 in.) was removed from the ball diameter during the lapping operation. Figure 6 depicts typical ball surfaces at the conclusion of the lapping process. The characteristics of the resultant surface were as anticipated and there are no signs of surface damage.

Table 1

Vicker's Hardness Data Measured on Silicon Nitride Billets

Billet Number	Hardness (kg/mm^2)	Billet Number	Hardness (kg/mm^2)
1280	1648	1292	1514
	1679		1545
	1679		1545
1281	1576	1293	1545
	1545		1545
	1545		1644
1282	1545	1294	1610
	1610		1610
	1610		1679
1284	1679	1295	1576
	1610		1545
	1610		1616
1285	1610	1296	1679
	1610		1679
	1644		1610
		1297	1679
			1610
			1610

average hardness   =   1607 kg/mm^2; 33 data points

standard deviation =   51 kg/mm^2

15

Table 2

Bulk Density of 34 Finished Silicon Nitride Balls

Density (g/cm^3)	Density (g/cm^3)
3.249	3.243
3.252	3.252
3.250	3.249
3.247	3.243
3.250	3.254
3.252	3.249
3.245	3.249
3.251	3.249
3.240	3.250
3.247	3.269
3.249	3.266
3.237	3.250
3.237	3.247
3.270	3.240
3.252	3.252
3.251	3.239
3.250	3.251

average density   =   3.25 g/cm^3; 34 data points

standard deviation =   0.008 g/cm^3

Figure 6. Photomicrographs of ... after ... scratch ...

Balls lapped with ... Si ...

8895   .25 in   8846   .5 in
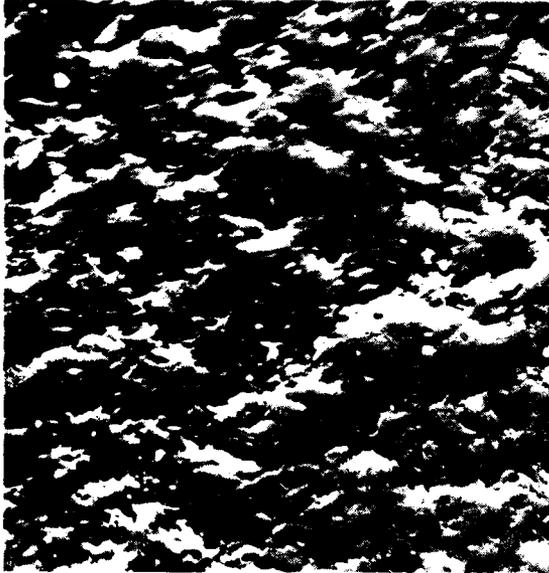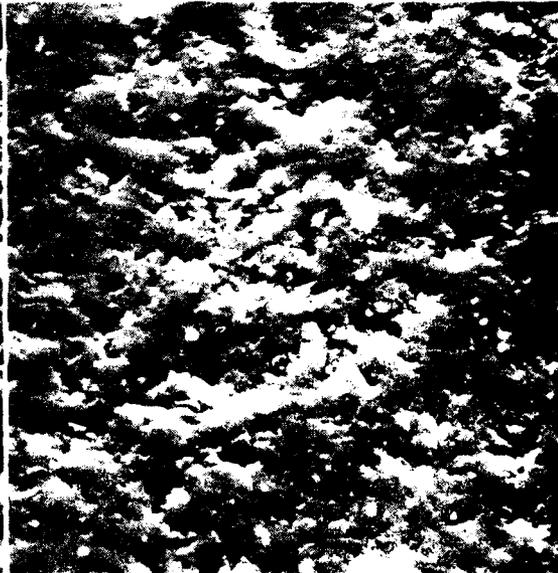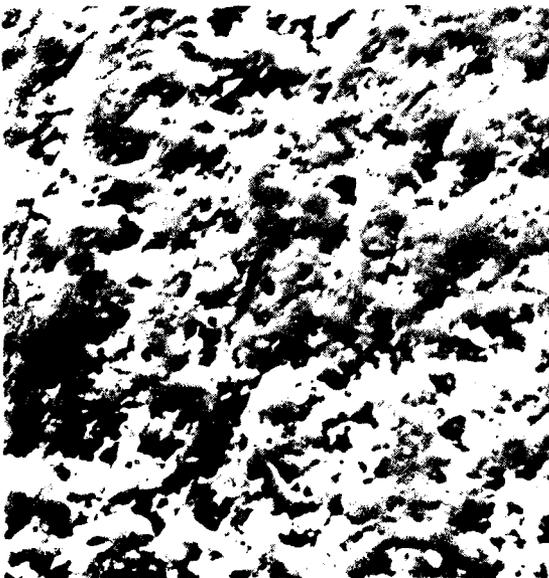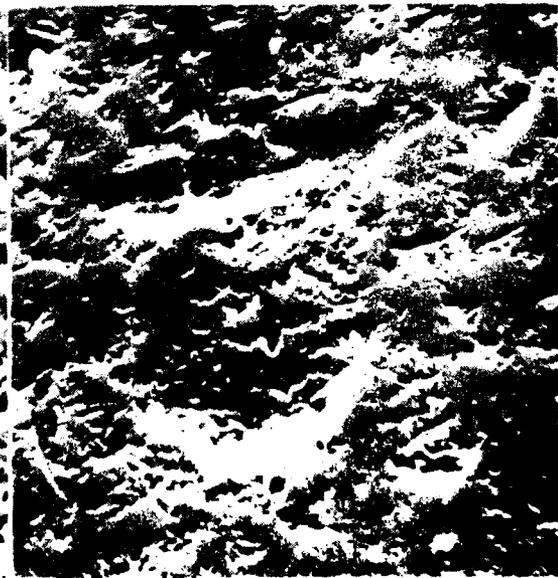
After rough lapping, the balls were finish polished in a
SGPL machine with 0.25 µm (1 x 10^{-5} in.) diamond abrasive.
Approximately 75 balls were processed simultaneously in each
SGPL load until the desired surface finish level was achieved.
These ceramic ball finishing procedures had been previously
developed through a number of NAVAIR sponsored programs [7,8].
After polishing, the balls conformed to AFBMA Grade 25 quality
requirements specified for the test bearings. Grade 25 balls
have a maximum allowable 2-point out-of-roundness of 0.64 µm
(25 x 10^{-6} in.) and a maximum surface roughness of 0.02 µm AA
(1 x 10^{-6} in. AA).

Figure 7 presents scanning electron micrographs of the final
polished silicon nitride balls. Note that unlike the balls used
in the previous program [16], no evidence of interconnected
porosity was observed on the ball surfaces during examination in
the scanning electron microscope. This observation attests to
the improved quality of balls manufactured from billets as com-
pared to those obtained from near-net shape silicon nitride
blanks. All of the features seen in these photomicrographs, i.e.
micropits and grinding lines, are typical of properly finished
silicon nitride balls.

### 3.2.5 Nondestructive Evaluation of Silicon Nitride Balls

The 962 finished silicon nitride balls were 100% inspected
with fluorescent dye penetrant using the procedures developed
under a program sponsored by the U.S. Air Force Materials Labor-
atory [15]. A sensitive flourescent dye penetrant (Zyglo ZL30;
ZR-10A) was used to impregnate the balls which were then inspected
visually under ultra-violet light.

Forty-three silicon nitride balls had fluorescent dye pene-
trant indications. The indications were circled with water
resistant ink and balls with indications were placed in a
separate lot for further analysis. Optical examination of the
rejected balls at magnifications up to 30X established that
twenty-three of these were false indications; organic material
on the ball surface had produced the indications. These balls
were returned to the main lot for use in the program. Table 5
contains a listing of the defect types noted on the remaining
twenty silicon nitride balls. Eleven balls had defects with
subtle indications which could not be easily characterized
optically. These balls were also rejected since the high yield
had provided the number of balls required for the program.

Figure 7. Photomicrographs of Finished Ball Surfaces.
Balls polished with 0.25 m Diamond Compound

8850   2500x

8853   2500x

19
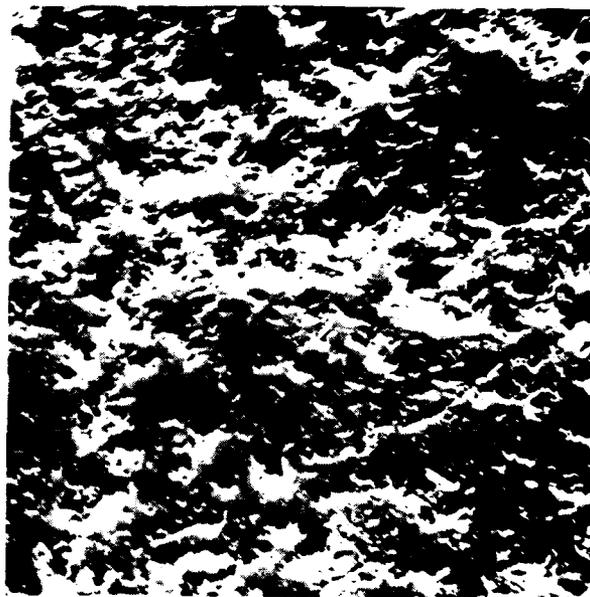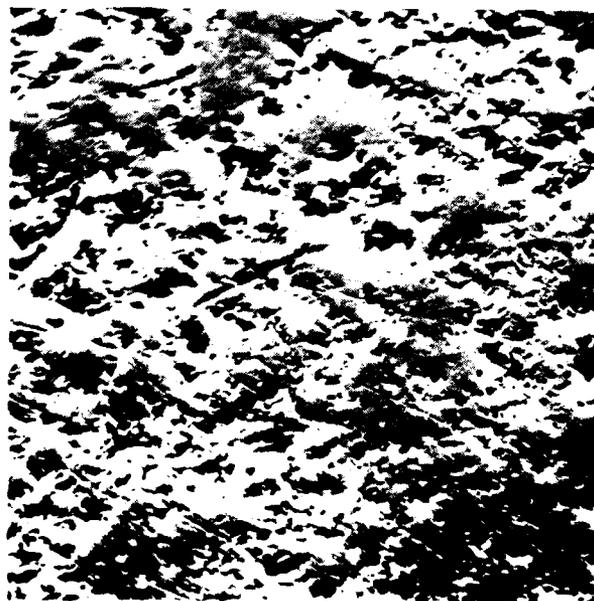
Figure 7. Photomicrographs of Finished Ball Surfaces.
Balls polished with 0.25 m Diamond Compound
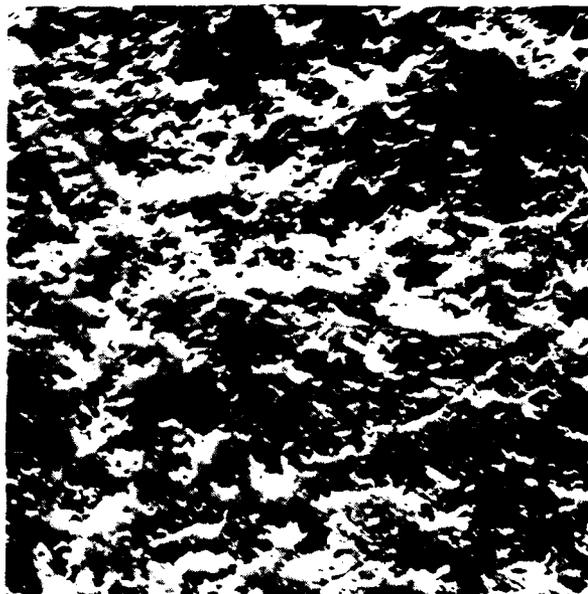
8850 2500x
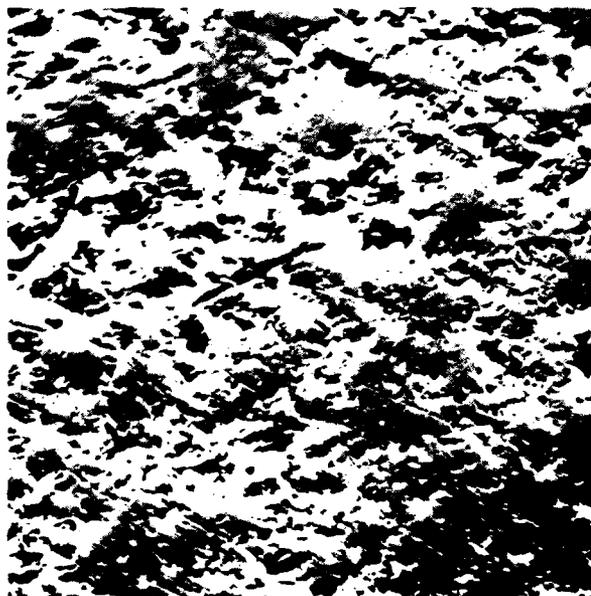
8853 2500x

19

Table 3

Defect Types Found By Dye Penetrant Inspection
of Finished Silicon Nitride Balls

Defect Type	Number of Balls Rejected
Cracks	3
Microporosity	2
Flat Spots/Chip Outs	2
Inclusions	2
Uncharacterized	<u>11</u>
Total	20

The results of this inspection process graphically illustrate
that the quality of the billet pressed silicon nitride material
is significantly better than that of the near net shape ceramic
material used in the preceeding program [16]. While those balls
had not been subjected to this inspection, a lot of 7 mm (0.276 in)
diameter balls had concurrently been manufactured from near net
shape parts for use in an AFML program [15]. After the early
ball failures were experienced in the hybrid bearing life tests,
this latter lot of balls was subjected to fluorescent dye penetrant
inspection. The average indication rate for material related
defects experienced at that time was 1 defect for every 18.1 cm^2
(2.8 in^2) of surface area. Since these defects were of the same
type and occurred at the same general frequency as those seen in
the failed 12.7 mm (0.50 in.) balls, it can be assumed that the
inspection of the earlier near net shape life test balls would have
shown a similar indication rate. In comparison, the indication
rate experienced in the current program was 1 defect in 1226 cm^2
(190 in^2) of surface area or one sixteenth of that previously
observed. These data should not be extrapolated to imply that
near net shape processing is technically unfeasible. However,
they do demonstrate the clear superiority of billet processed
ceramic material at the current level of technological development.

4. TEST EQUIPMENT

The test machines used in the experimental investigation were standard SKF owned R2 type bearing endurance testers. Specialized test hardware was provided to accommodate 7209 size angular contact 'all bearings under pure thrust load. The test arrangement is shown photographically in Figure 8 and illustrated graphically in the layout drawing of Figure 9.

Basically, the machine consists of a hollow horizontal arbor which is supported on a rigid cast base by two cylindrical roller bearings. The arbor is belt driven through a centrally located pulley by a constant speed AC motor. The pulley ratio yields a test speed of 1016 rad/s (9700 rpm).

A test bearing is mounted near each end of the shaft outboard of the load bearing support points. Each test bearing is enclosed in an independent floating housing to minimize the interaction between test bearing assemblies. The alignment of the test housing, and thus the test bearing, is controlled relative to the shaft by a small cylindrical pilot bearing located at the extreme end of the arbor.

Axial load is applied to the two test bearings by means of a tensioned rod passing through the center of the hollow shaft and connecting the floating housings. A strain gage transducer at one end of the rod allows the magnitude of the applied load to be directly measured.

Lubrication is provided to the bearings from a centrally located supply system. The lubricant used in these tests was a commercially available ester based synthetic fluid meeting the MIL-L-23699 specification. The circulating system is equipped with a 25 μm full flow filter to remove any debris from the fluid before it is delivered to the bearings. A water cooled, thermostatically modulated heat exchanger is employed to maintain the lubricant supply temperature below 311K (100°F). The specific flow rate to each bearing is controlled by a flow meter to control the bearing operating temperature within a specified range.

The test machine is equipped with a vibration sensitive shut-off transducer. An increase in the general bearing vibration level is indicative of a spalling fatigue failure of a bearing component. When an increase is sensed by the transducer, the test machine is shutdown automatically to prevent the progression of the damage and the loss of failure initiation data.

Figure 8

Photographic View of R2 Endurance Tester
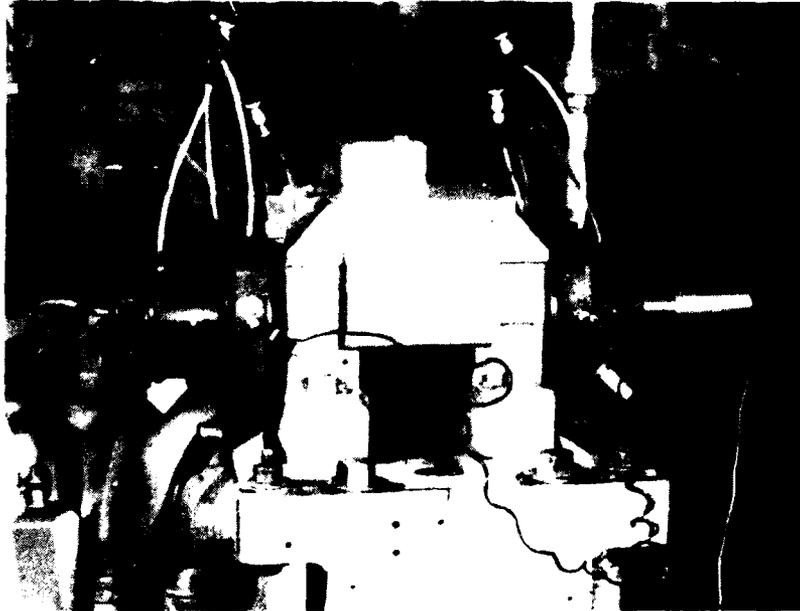
Figure 9

Schematic Layout of 7209 Test Arrangement
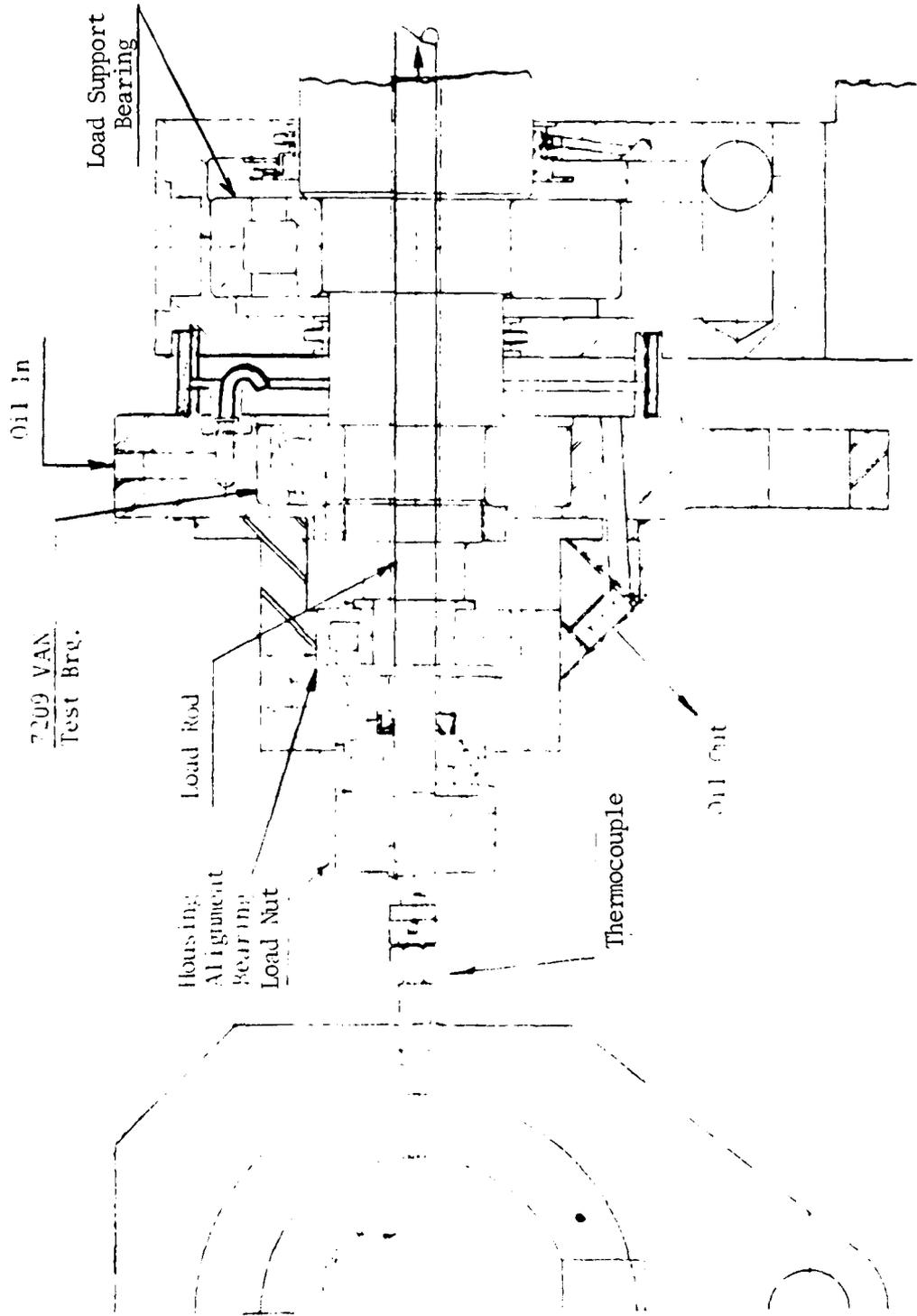
Thermocouples are located in the housings to measure the outer ring operating temperature of the test bearings. The analog signals from these sensors, as well as those from the load transducers, are monitored by a Test Floor Control System which contains a Nova 800 digital computer as a central processing unit. The control system constantly scans the data input points at a rate sufficient to provide less than a 2 second interval between consecutive readings on any one point. Each scan, the value of every point is compared against individual preestablished limits and if the point is outside this range, an alarm message is activated. If the value exceedes a higher preset limit, the system will automatically shut the test machine off. In addition to these control functions, the system can accumulate a histor- ical record of the data on specified points designated whole minute intervals.

5. EXPERIMENTAL RESULTS

The test plan was established to define the load-life relationship of the specially designed steel/ceramic hybrid 7209 VAN angular contact ball bearings. This was to be accomplished by conducting endurance tests on three groups of twenty bearings each at three different load levels. The magnitudes of the applied thrust loads were calculated to produce inner ring maximum Hertz stress levels identical to those in all steel bearings at C/P values of 2.15, 3.0 and 3.75. The established test plan also would allow the definition of a preliminary value of an a_2 material factor for use in calculating the life of hybrid bearing assemblies. This information would be available as a function of the ratio between the experimentally achieved bearing lives and the theoretically predicted values, considering an appropriate value of the a_3 application factor. To date, testing has been completed on two 10 bearing groups at the high and low load levels.

Endurance testing was initiated at the highest planned axial load of 9.56 kN (2150 lbf). This load produces an inner ring maximum Hertz stress level of 2.44 GPa (3.54 x 10^5 psi) and a theoretical bearing life of 15 x 10^6 revolutions. For these tests, the speed was 1016 rad/s (9700 rpm) and the MIL-L-23699 lubricant was supplied at a rate sufficient to control the bearing outer ring operating temperature at 333 to 338K (60-65°C). At this operating temperature, the calculated value of the lubricant film parameter Λ is 2.9.

Three of the nine bearings placed on test suffered spalling failures of the ceramic balls at lives ranging from 14.5 x 10^6 to 76.2 x 10^6 revolutions. In addition, two combination inner ring, outer ring, ball failures were experienced at lives of 25.6 x 10^6 and 33.1 x 10^6 revolutions. A statistical analysis of these failure data, listed in Table 4, completed by the maximum likelihood technique, establishes the experimental L_{10} life as 18.5 x 10^6 revolutions. Testing was suspended at this point.

The tested bearing components were examined visually at magnifications up to 30X. The appearance of the unfailed bearings was quite good; the contact surfaces remained in excellent condition and the load track was properly located. Typically, the remaining balls in the failed bearings also appeared extremely good. In fact, it was difficult to find any evidence of running on the unfailed balls even though a considerable amount of debris would have been present in the bearings as a result of the failure. The failures were analyzed in detail and

Table 4

7209 VAN Hybrid Bearing Test Data Accumulated
Under High Load

Speed: 1016 rad/s (9700 rpm)

Axial Load: 9.56 kN (2150 lbf)

Lubrication: Circulating Mobil Jet II Synthetic Fluid
(MIL-L-23699)

Bearing No.	Life 10^6 Revolutions	Mode of Failure
46	69.3	Suspended
53	52.4	Suspended
54	14.5	1 Spalled Ball
56	76.2	1 Spalled Ball
57	33.1	Combination Inner Ring, Outer Ring, 1 Ball
72	32.0	Suspended
81	25.6	Combination Inner Ring, Outer Ring, 3 Balls
82	66.3	1 Spalled Ball
87	69.8	Suspended

Basic Rating Life: $L_{10} = 15 \times 10^6$ Revolutions

Experimental $L_{10} = 18.5 \times 10^6$ Revolutions

the results are reported in Section 6.

The second eleven bearing test group was run at a thrust load of 5.0 kN (1125 lbf) which had been calculated as the lowest load to be used in the load-life series. This load produces a maximum inner ring Hertz stress of 2.0 GPa (2.9×10^5 psi) and a theoretical bearing L_{10} life equal to 73×10^6 revolutions. The operating temperature of the bearing was reduced to 323 to 328 K (50-55°C) in recognition of the lower heat generation rate of this lower load. The reduced operating temperature and the reduction in applied load increased the calculated value of Λ to 4.1 for this group. The difference between this lubrication condition and that existant in the high load group which had a Λ of 2.9 is probably not significant. If these were steel bearings, the values of the a_3 application condition life modification factors produced by these Λ values would be 2.3 and 2.4 respectively using the ASME recommended relationship [20]. It would be expected then that a variation in film parameters of this magnitude would also have a minor effect on the life of hybrid bearing assemblies. The remaining test conditions were identical to those used in the first group.

Three combination inner ring, outer ring, one ball failure were experienced at lives of 217×10^6, 281 a 10^6 and 561×10^6 revolutions. Concurrently, six bearings achieved lives in excess of 400×10^6 revolutions without failing, while the remaining two were suspended earlier for operational reasons also without failing. The statistical evaluation of the failure data displayed in Table 5 provided an estimate of the experimental L_{10} equal to 248×10^6 revolutions, 3.4X the basic theoretical value.

These failures were also examined in detail and the results are presented in Section 6.

28

Table 5

7209 VAN Hybrid Bearing Test Data Accumulated
Under Low Load

Speed: 1016 rad/s (9700 rpm)

Axial Load: 5.0 kN (1125 lbf)

Lubrication: Circulating Mobil Jet II Synthetic Fluid
             (MIL-L-23699)

Bearing No.	Life 10^6 Revolutions	Mode of Failure
05	700	Suspended
20	700	Suspended
45	561	Combination Inner Ring, Outer Ring, 1 Ball
49	411	Suspended
50	217	Combination Inner Ring, Outer Ring, 1 Ball
51	414	Suspended
52	414	Suspended
60	281	Combination Inner Ring, Outer Ring, 1 Ball
83	86	Suspended
85	236	Suspended
86	499	Suspended

Basic Rating Life: $L_{10} = 73 \times 10^6$ revolutions

Experimental $L_{10} = 248 \times 10^6$ revolutions

6. ROLLING ELEMENT FAILURE ANALYSIS

6.1 Introduction

The silicon nitride balls which underwent life testing were subjected to intensive failure analysis using optical and scanning electron microscopy. General ball surface appearance, fracture origins, and spall progression were documented by these techniques. In addition, x-ray diffraction was used in an attempt to determine if fracture initiated in a preferred direction related to the hot pressing direction. No evidence of material defects or of a preferred plane of "weakness" related to the hot pressing direction were found during the analysis.

6.2 Optical Analysis

Optical analysis of the spalled silicon nitride ball was the first step in failure analysis. Fracture origins and crack propagation directions were readily observed during optical inspection. Figure 10 shows typical silicon nitride ball spalls. Note that the general surface appearance was similar among balls tested at two different thrust loads; ball 618-050 at 5.0 kN (1125 lbf); and balls 610-054, 610-056, and 610-057 at 9.56 kN (2150 lbf). After locating fracture origins, selected balls were observed by the scanning electron microscope.

6.3 SEM Analysis

Fracture origins, and general surface conditions were evaluated using secondary electron and backscattered electron imaging techniques. SEM analysis of fracture origins did not detect any material inclusions, porosity, or other defects which would act as stress concentrators and initiate premature failure of the balls. Fracture originated at cone cracks due to stress. Unlike the previous program [16], all fracture origins analyzed were free from material defects further illustrating the improvements in material quality that was achieved.

Figures 11 and 12 contain scanning electron photomicrographs at various magnifications of spall initiation areas on two balls tested at the high load. Figure 13 is a composite sequence of photomicrographs documenting fracture initiation and presumed spall progression from a series of balls also tested at the high load. Figure 13A shows a typical cone crack which is thought to be the failure initiation point. Figures 13B, 13C and 13D show the progression of this crack into extensively spalled areas in the direction of the maximum stress. Figure 13D also illustrates

Figure 19. [illegible] ogical [illegible] n Tested
Silicon Nitride [illegible]
[illegible] Spall Ori[illegible] [illegible]licate
[illegible]ll Propagation [illegible]

618-[illegible]: [illegible] hours
5kN [illegible]

618-051: 25 [illegible]
9.50 kN [illegible]

Figure 11. ...ion Direction
No. 82

Figure 12. Fracture [illegible] [illegible] [illegible] [illegible] [illegible]ation Direction
          In [illegible] [illegible] [illegible] [illegible] [illegible] [illegible]rin No. 56
          [illegible] [illegible] [illegible]

9086 20X 618-056 131HR SI3N4

9087 75X 618-056 131HR SI3N4

Figure 1.

A — 9081 75X 618-082 114HR SI3N4

B — 9093 75X 618-081 44HR SI3N4

Hertzian cracking initiation

C — 9096 30X 610-057 45HR SI3N4

D — 9091 30X 618-081 44HR SI3N4

spall propagation on the concave side of the original crack. This progression results from the continued impact at the discontinuity in the silicon nitride surface. A small semicircular crack can be seen at the edge of the spalled area in Figure 13C. Continued running would have resulted in the growth of a spalled region at this juncture also.

Figure 14 shows the surfaces of two unfailed silicon nitride balls after 45 and 131 hours (33.1 and 76.2 x 10^6 revolutions) of testing at the high thrust load level. The general surface appearance of these balls is similar to that of the untested balls shown previously in Figure 5. Figure 15 shows the surfaces of two silicon nitride balls which accumulated more than 700 hours (400 x 10^6 revolutions) without failure at the low load level. The appearance of these components is also comparable to that of the untested balls.

Figure 16 shows the spall origin in a silicon nitride ball and an M50 outer ring spall, both from bearing 060. This bearing failed after 484 hours of operation at the low load. The silicon nitride spall origin is similar to these noted in the high load tests as illustrated with the comparison of Figures 13 and 16. Again no inclusions were dete ted at the fracture origin.

The outer race spall shown in Figure 16 is not typical of the failures seen previously on steel components from hybrid bearings. In all previous cases, the failure of the steel part occurred in conjunction with a ceramic component failure which was thought to cause the ring failure. The steel races in those instances showed plastic deformation, general areas of denting, and deep narrow spalls oriented across the groove. While the current spall was also found in a bearing with a ball failure, the appearance of the spall was more typical of that seen in an all steel bearing. It is therefore possible that the ring spall preceeded the ball failure in this specific bearing.

Figure 14. Photo... ...con Nitride Ball

Figure 15. Photomicrographs of Unfailed Silicon Nitride Ball
Surfaces Run Under 1g Load
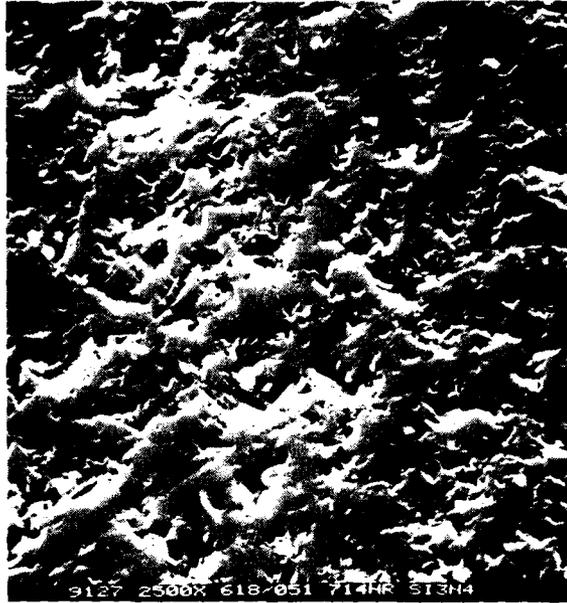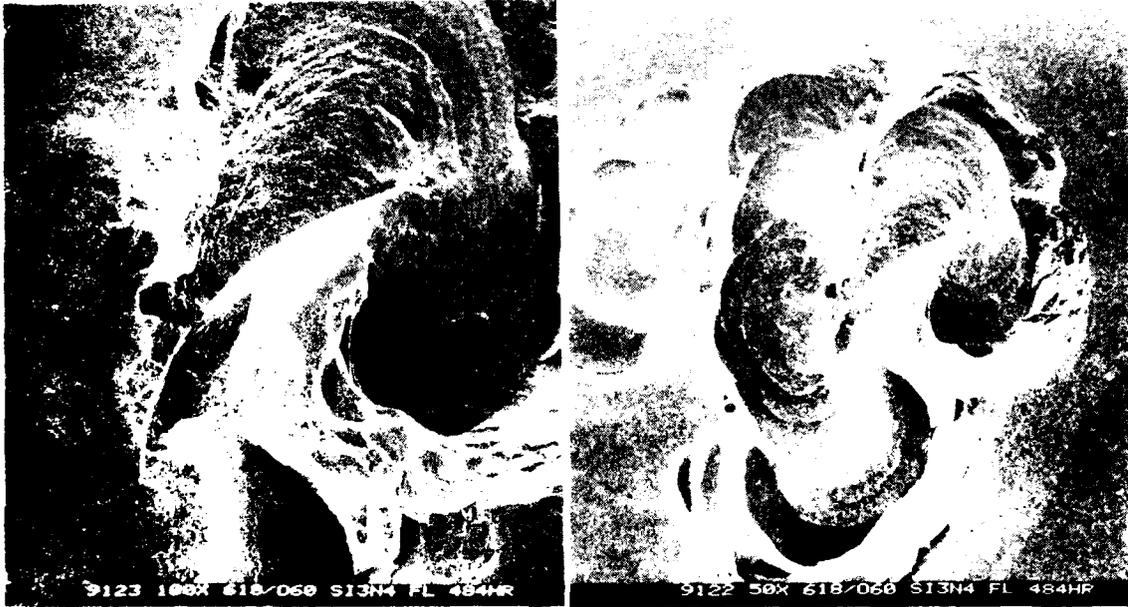
Balls from Bearing 51
5.0 kN Test Load; 714 Test Hours

Figure ... Photomicrographs of Ball Fracture Origin and Outer
Ball ... all Run Under Low Load
... ...: 484 Hours

7. DISCUSSION OF RESULTS

Spalling failures were experienced in eight of the twenty bearings tested. Three of these were ball failures, while the remaining five failures were comprised of spalls on both steel race surfaces and at least one ceramic ball. It was apparent from visual examination that four of the five combination failures had initiated on the rolling elements. The remaining failure, that which occurred after 281×10^6 revolutions at the low load, could have initiated on the outer ring or the ceramic ball. Nonetheless, the distribution of the failure data illustrates that, at least at this time, the ceramic rolling element is the most critical component in a hybrid angular contact bearing. This is opposed to experience accumulated in steel bearings where most failures initiate on the inner rings.

Further failure analysis conducted using scanning electron microscopy indicated that the ball failures had been initiated by cone shaped cracks, a well defined ceramic failure mode. These cracks initiate at the surface of the ceramic material as a result of radial tensile stresses created at the edges of the contact zone. Further stress cycles forced the cracks to progress into the material to form a spall. No evidence of the presence of voids or inclusions was found in the examination of the ceramic material. It is concluded that the ceramic material used in this program was of bearing quality and the spalls experienced were valid fatigue originated failures.

The experimental L_{10} lives of the test lots, i.e. 18.5×10^6 and 248×10^6 revolutions for the high and low load groups respectively, are approximately 5 times greater than those achieved in the previous program. Additionally, the ratios of the experimental results to the Lundberg-Palmgren theoretical lives are 1.2 for the high load group and 3.4 for the low load group. These results are very positive indicating that steel/ceramic hybrid bearings can achieve viable life expectancies even under these endurance test level loads which are significantly higher than what would be encountered in a practical application.

These life results also imply that the load-life relationship for hybrid bearings may be different from that of steel bearings i.e. the exponent p used in the life formula may not be equal to 5. Of course, the data available are insufficient to establish magnitude of the exponent and the form of this relationship. However, within the load range of the test series, it appears

that the hybrid design is more sensitive to increases in the magnitude of the applied load. Whether this observation is reflective of the overall form of the load life relationship or has resulted from the overloading of the ceramic elements at the highest load level will only become obvious with further testing.

Life comparisons between hybrid and steel bearings are difficult to achieve at this time due to a lack of data. The analytical work completed in [16] established that the hybrid bearing has a significant life advantage for high speed applications at practical load levels. However, at the low speed, high load levels of this endurance test series, the steel bearings have a theoretical life advantage. These calculations were completed without the use of life modification factors so that variations in a_2a_3 values for these bearings affect the real life comparisons. Past experience [21] has shown that for VimVar M50 material an a_2 factor of five can be employed. The small amount of life data collected to date on the hybrid bearing shows an apparent a_2a_3 factor ranging from 1.2 to 3.4 for the hybrid bearing. The trend of the results is that the apparent a_2a_3 factor increases as the applied load is decreased. If this very preliminary result is supported by subsequent testing, the hybrid bearings will provide the theoretically calculated life advantages in high speed systems like aircraft gas turbine engines.

Once again, the silicon nitride rolling elements displayed a considerable degree of durability in this test program. Spalled balls did show a tendency for the spalls to progress with subsequent running. However, the degree of spall progression noted would be considered normal for a steel ball. There were no instances where the total surface of the ceramic ball was removed or where fracture initiated from the initial spall. Even in those bearings with raceway spalls where the balls would have been subjected to severe impact loads passing over the failed area, the ceramic elements showed no tendency for uncontrolled spalling or cracking.

The surfaces of unfailed balls appear to be comparable to that of new balls regardless of the amount of running time accumulated. This is true even for those balls taken from bearings having failures. In comparison, the steel raceways of bearings containing a failed element showed extensive amounts of denting and abrasive wear.

8. CONCLUSIONS

1. Hybrid angular contact ball bearings, having steel rings and silicon nitride ceramic rolling elements, are capable of achieving experimental lives in excess of those predicted by Lundberg-Palmgren theory even when subjected to loads much higher than those used in practical applications.

2. The load life behavior of hybrid bearings is possibly different than that of all steel bearings under the range of conditions employed in this program. Currently, this relationship can not be defined since insufficient life data exist.

3. Ceramic rolling elements are sufficiently durable to resist fracture, parasitic spalling, and debris initiated surface deterioration even when operating in a heavily loaded bearing containing spalled areas and failure debris.

4. The ceramic rolling elements selected for use in these test bearings contained no apparent raw material or process related defects, so the failures were generated by a conventional ceramic fracture mode.

9. RECOMMENDATIONS

The results achieved in this program to date are extremely favorable. The potential for hybrid ceramic/steel angular contact ball bearings to achieve practically acceptable service lives has been demonstrated under very high loads. These results justify the continued evaluation of these experimental bearings to generate the design principles necessary for their usage in practical systems. Specifically, additional experimental life data needs to be accumulated at a variety of loads to allow the establishment of preliminary values of the exponent p in the load-life relationship, and the a_2a_3 life adjustment factors. In addition, life testing is required at high speeds to demonstrate the theoretical life advantage that hybrid bearings have over steel bearings at these operating conditions. It is currently planned that data will be obtained in both of these areas in an existing follow on effort.

Furthermore, continued investigation of ceramic forming and processing methods as a means of reducing manufacturing costs would also seem to be warranted. Nondestructive test techniques suitable for production use should also be pursued as a means of assuring the quality of ceramic bearing components.

10. REFERENCES

1. Chiu, Y.P. and Dalal, H. M., "Lubricant Interaction with Silicon Nitride in Rolling Contact Applications", Symposium on Ceramics for High Performance Applications, Army Mechanics and Materials Research Center,(November, 1973.)

2. Dalal, H. M., Chiu, Y. P. and Rabinowicz, E., "Evaluation of Hot Pressed Silicon Nitride as a Rolling Bearing Material", ASLE Trans. 18 (3) 211-221 (1975).

3. Dalal, H. M., et al, "Evaluation of Hot Pressed Silicon Nitride as a Rolling Bearing Material", NASC-ONR R & D Program Review on Silicon Nitride as a Bearing Material (1974).

4. Wheildon, W. M., Baumgartner, H. R., Sundberg, D. V., and Torti, M. L., "Ceramic Materials in Rolling Contact Bearings", Final Report on NAVAIR Contract N00019-72-C-0299, Jan. 1972 to Feb. 3, 1973. (1973)

5. Baumgartner, H. R. and Wheildon, W. M., "Rolling Contact Fatigue Performance of Hot-Pressed Silicon Nitride Versus Surface Preparation Techniques", in Materials Science Research 7, Frechette, V. D., LaCourse, W. C. and Burdick, V.L., edit. Plenum Press, New York and London,(1974.)

6. Dalal, H. M., et al, "Effect of Surface and Mechanical Properties on Silicon Nitride Bearing Element Performance," SKF Report No. AL75T002, Final Report on Naval Air Systems Command,Contract N00019-74-C-0168 (February, 1975).

7. Dalal, H. M., et al, "Effect of Lapping Parameters on Generation of Damage on Silicon Nitride Ball Surfaces," SKF Report No. AL76T026, Final Report on U. S. Department of the Navy Contract No. N00019-76-C-0147 (December, 1976).

8. Dalal, H. M, et al, "Development of Basic Processing Technology for Bearing Quality Silicon Nitride Balls," SKF Report AL77T057, Final Report on U. S. Department of the Navy Contract No. N00019-76-C-0684 (1977).

9. Baumgartner, H. R., "Evaluation of Roller Bearings Containing Hot Pressed Silicon Nitride Rolling Elements," Second Army Materials Technology Conference, Ceramics for High Performance Applications,(Nov. 1973.)

10. Dalal, H. M. et al, "Surface Endurance and Lubrication of Silicon Nitride Ball Bearings," Final Report on U. S. Department of the Navy Contract No. N00019-75-C-0216, SKF Report AL75T030 (December, 1975).

11. Morrison, F. R., and Sibley, L. B., "Application of Ceramic Ball Bearings to the MERADCOM 10 KW Turbine", SKF Report No. AL77T033, Phase I Final Report on Solar P. O. No. 6981-24131-M35, Subcontract to U.S. Army Mobility Equipment Research and Development Command, Contract DAAG53-76-C-0228 (1977).

12. Baumgartner, H. R., Sundberg, D. V., and Wheildon, W. M., "Silicon Nitride in Rolling Contact Bearings", Final Report on NAVAIR Contract N00019-73-C-0193, Jan. 3 to Oct. 3, 1973 (1973).

13. Parker, R. J. and Zaretsky, E. V., "Fatigue Life of High-Speed Ball Bearings With Silicon Nitride Balls", ASME Paper No. 74-Lub-12, ASME-ASLE Joint Lubricaton Conference, Montreal, Canada, October 1974.

14. Valori, R., "Rolling Contact Fatigue of Silicon Nitride", Naval Air Propulsion Test Center Report No. NAPTC-PE-42, (August 1974.)

15. Scilingo, A.A., "Manufacturing Methods for Ceramic Bearing Components", U. S. Air Force, AFSC Aeronautical Systems Division, Contract F33615-78-C-5010, SKF Report AL79M019.(1979)

16. Morrison, F. R., Pirvics, J, and Yonushonis, T., "Establishment of Engineering Design Data for Hybrid Steel/Ceramic Ball Bearings", U. S. Department of the Navy, Naval Air Systems Command, Contract N00019-78-C-0504, SKF Report AL79T033 (September, 1979).

17. Lundberg, G. and Palmgren A., "Dynamic Capacity of Rolling Bearings", Acta Polytechnica, Mechanical Engineering Series 1, Proceedings of the Royal Swedish Academy of Engineering, Vol. 7, No. 3, (1947).

18. Lundberg, G. and Palmgren A., "Dynamic Capacity of Roller Bearings", Proceedings of the Royal Swedish Academy of Engineering, Vol. 2, No. 4, (1952).

19. ANSI/AFBMA Standard 11-1978 "Load Ratings and Fatigue Life for Ball Bearings" (1978).

20. Bambarger, E. N. et.al., "Life Adjustment Factors for Ball and Roller Bearings, An Engineering Design Guide", American Society of Mechanical Engineers, New York, N. Y. (1971).

21. Morrison, F. R., McCool, J. I. and Ninos, N. J., "M50 Steel Bearing Material Factors for Rolling Element Life Calculations - Phase II", U. S. Army Aviation Research and Development Command, Contract DAAK50-78-C-0027 AVRADCOM TR79-48 (1979).

APPENDIX A
NORTON RAW MATERIAL CERTIFICATION DATA

POWDER LOT HN-15
BILLETS 1280   1285, 1292   1297,
AND 1307

Table A-1

X-Ray Radiographic Results and Density of Norton NC132
Hot Pressed Silicon Nitride

Billet Number	Density	Norton X-Ray No. *
1280	3.28	MMR-G21-33
1281	3.29	MMR-G21-33
1282	3.29	MMR-G21-33
1283	3.30	AG-B20909
1284	3.26	AG-B20909
1285	3.27	AG-B20909
1292	3.27	AG-B20917
1293	3.26	AG-B20917
1294	3.26	AG-B20917
1295	3.26	MMR-G30-3
1296	3.26	MMR-G30-3
1297	3.27	MMR-G30-3
1307	3.26	MMR-G37-6

$$\text{AVE} = 3.27$$
$$\text{S.D.} = 0.01$$

* Radiographic inspection showed no abnormalities.

47

Table A-2

Certification of Powder Lot HN-15 - Chemical Analysis

Element	Percent
Mg	0.94
Ca	0.03
Fe	0.29
Al	0.20
O_2	3.70
W	2.40

48

Table A-3
Certification of Powder Lot HN15 - Mechanical Properties

A.   Room Temperature Four Point Flexure Strength

ksi	(MPa)
135.4	(933.6)
134.3	(926.0)
132.5	(913.6)
131.9	(909.5)
128.5	(886.0)
107.4	(740.5)
106.8	(736.4)
105.7	(728.8)
$\bar{x}$ = 122.8	$\bar{x}$ = (846.7)
S.D. = 13.6	S.D. = (93.8)

B.   2500°F (1370°C) Three Point Flexure Strength

ksi	(MPa)
47.6	(328)
46.9	(323)
45.4	(313)
44.6	(308)
$\bar{x}$ = 46.1	$\bar{x}$ = (318)
S.D. = 1.4	S.D. = (10)

DISTRIBUTION LIST

<div align="right">No. of Copies</div>

Naval Air Systems Command   17
Washington, D.C.   20361
Attention: AIR 00D4   9
            310C   1
            330   1
            536   1
            320A   1
            5163D4   4

Office of Naval Research   1
Washington, D.C.   20360
Attention: Code 471

White Oak Laboratory   1
Naval Surface Weapons Center
White Oak, Maryland   20910
Attention: Code 2301

Naval Research Laboratory   1
Washington, D.C.   20390
Attention: Code 6360

David W. Taylor Naval Ship Research & Development Center   1
Annapolis, Maryland   21402
Attention: W. Smith, Code 2832

Naval Air Propulsion Center   1
Trenton, New Jersey   08628
Attention: R. Valori, Code PE 72

Naval Undersea Center   1
San Diego, California   92132
Attention: Dr. J. Stachiw

Naval Air Development Center   1
Materials Application Branch, Code 6061
Warminster, Pennsylvania   18974

Air Force Wright Aeronautical Laboratories   4
Wright-Patterson, Air Force Base
Dayton, OH 45433
Attention: Dr. J. Dill   POSL 1
           Dr. H. Graham   MLLM 1
           Mr. B. D. McConnell MLBT 1
           Ms. K. Lark   MLTM 1

Brookhaven National Laboratory   1
Upton, NY 11973
Attention: Dr. D. Van Rooyen

Director   1
Applied Technology Laboratory
U.S. Army Research & Technology Laboratories
Fort Eustis, Virginia 23604
Attention: DAVDL-ATL-ATP (Mr. Pauze)

U.S. Army Research Office   1
Box CM, Duke Station
Durham, North Carolina 27706
Attention: CRDARD

U.S. Army MERDC   1
Fort Belvoir, Virginia 22060
Attention: W. McGovern (SMEFB-EP)

Army Materials and Mechanics Research Center   1
Watertown, Massachusetts 02172
Attention: Dr. R. N. Katz

NASA Headquarters   1
Washington, D.C. 20546
Attention: J. J. Gangler, RRM

NASA Lewis Research Center   2
21000 Brookpark Road
Cleveland, Ohio 44135
Attention: Dr. E. Zaretsky   1
            W. A. Sanders (49-1)   1
               and Dr. T. Hergell

Defense Advanced Research Project Office   2
1400 Weilson Boulevard
Arlington, Virginia 22209
Attention: Dr. Van Reuth 1
            Dr. Buckley   1

Inorganic Materials Division   1
Institute for Materials Research
National Bureau of Standards
Washington, D.C. 20234

University of California   1
Lawrence Berkeley Laboratory
Hearst Mining Building
Berkeley, California 94720
Attention: Dr. L. Froschauer

Department of Engineering   1
University of California
Los Angeles, California 90024
Attention: Profs. J. W. Knapp and G. Sines

Department of Metallurgy   1
Case-Western Reserve University
Cleveland, Ohio 44106
Attention: Dr. A. Heuer

Engineering Experiment Station   1
Georgia Institute of Technology
Atlanta, Georgia 30332
Attention: J. D. Walton

Department of Engineering Research   1
North Carolina State University
Raleigh, North Carolina 27607
Attention: Dr. H. Palmour

Materials Research Laboratory   1
Pennsylvania State University
University Park, Pennsylvania 16802
Attention: Prof. Rustum Roy

Rensselaer Polytechnic Institute   1
110 Eighth Street
Troy, New York 12181
Attention: R. J. Diefendorf

School of Ceramics   1
Rutgers, The State University
New Brunswick, New Jersey 08903

Virginia Polytechnic Institute   1
Minerals Engineering
Blacksburg, Virginia 24060
Attention: Dr. D. P. H. Hasselman

Aerospace Corporation   1
Materials Laboratory
P.O. Box 95085
Los Angeles, California 90045

Supervisor, Materials Engineering   1
Department 93-39M
AiResearch Manufacturing Company of Arizona
402 South 36th Street
Phoenix, Arizona 85034

Materials Development Center AVCO System Division Wilmington, Massachusetts 01887 Attention: Tom Vasilos	1
Lycoming Division AVCO Corporation Stratford, Connecticut 06497 Attention: Mr. D. Wilson	1
Barden Corporation Danbury, Connecticut 06810 Attention: Mr. K. MacKenzie	1
Batelle Memorial Institute Ceramics Department 505 King Avenue Columbus, Ohio 43201	1
Metals and Ceramics Information Center Batelle Memorial Institute 505 King Avenue Columbus, Ohio 43201	1
Bell Helicopter Textron P. O. Box 482 Fort Worth, Texas 76101 Attention: R. Battles	1
The Boeing Company Materials and Processes Laboratories Aerospace Group P. O. Box 3999 Seattle, Washington 98124	1
Research and Development Division Carborundum Company Niagara Falls, New York 14302 Attention: Mr. C. McMurty	1
Caterpillar Tractor Company Technical Center East Peoria, Illinois 61611 Attention: A. R. Canady	1
Ceramic Finishing Company Box 498 State College, Pennsylvania 16801	1
Ceradyne, Inc. Box 1103 Santa Ana, California 92705	1

Coors Porcelain Company   1
600 Ninth Street
Golden, Colorado 80401
Attention: Research Department

Cummings Engine Company   1
Columbus, Indiana 47201
Attention: Mr. R. Kamo, Director of Research

Curtiss-Wright Company   1
Wright Aeronautical Division
One Passaic Street
Wood-Ridge, New Jersey 07075

Fafnir Bearing Company   1
Division Textron Corporation
27 Booth Street
New Britain, Connecticut 06050

F.A.G. Bearing Corporation   1
70 Hamilton Avenue
Stamford, Connecticut 06904
Attention: Joseph Hoo

Federal-Mogul Corporation   1
Anti-Friction Bearing R&D Center
3980 Research Park Drive
Ann Arbor, Michigan 48104
Attention: D. Glover

Product Development Group   1
Ford Motor Company
20000 Rotunda Drive
Dearborn, Michigan 28121
Attention: Mr. E. Fisher

Aircraft Engine Group   1
Technical Information Center
Main Drop N-32, Building 700
General Electric Company
Cincinnati, Ohio 45215

Metallurgy and Ceramics Research Department   1
General Electric R&D Laboratories
P.O. Box 8
Schenectady, New York 12301

Space Sciences Laboratory   1
General Electric Company
P.O. Box 8555
Philadelphia, Pennsylvania 19101

54

Detroit Diesel Allison Division   1
General Motors Corporation
P.O. Box 894
Indianapolis, Indiana 46206
Attention: Dr. M. Herman

NDH Division   1
General Motors Corporation
Hayes Street
Sandusky, Ohio
Attention: H. Woerhle

Hughes Aircraft Company   1
Culver City, CA 90230
Atention: M. N. Gardos

IIT Research Institute   1
10 West 35th Street
Chicago, Illinois 60616
Attention: Ceramics Division

Industrial Tectonics, Inc.   1
18301 Santa Fe Avenue
Compton, California 90224
Attention: Hans R. Signer

Kaweki-Berylco Industry   1
Box 1462
Reading, Pennsylvania 19603
Attention: Mr. R. J. Longnecker

Research and Development Division   1
Arthur D. Little Company
Acorn Park
Cambridge, Massachusetts 02140

Mechanical Technology, Inc.   1
968 Albany-Shaker Road
Latham, New York 12110
Attention: Dr. E. F. Finkin

North American Rockwell Science Center   .   1
P.O. Box 1085
Thousand Oaks, California 91360

Rollway Bearing Company   1
Division Lipe Corporation
7600 Morgan Road
Liverpool, New York 13088
Attention: B. Dalton

Pratt & Whitney Aircraft Division   1
United Aircraft Corporation
East Hartford, Connecticut   06108
Attention: Paul Brown   EB-2

Pratt & Whitney Aircraft Division   1
United Aircraft Corporation
Middletown, Connecticut   06108
Attention: L. E. Friedrich, MERL

Pratt & Whitney Aircraft Division   1
United Aircraft Corporation
Florida R&D Center
West Palm Beach, Florida
Attention: Mr. J. Miner

Astronuclear Laboratory   1
Westinghouse Electric Corporation
Box 10864
Pittsburg, Pennsylvania   15236

Westinghouse Research Laboratories   1
Beulah Road
Churchill Borough
Pittsburgh, Pennsylvania   15235
Attention: Dr. R. Bratton

Williams Research Corporation   1
Walled Lake, Michigan   48088

Litton Guidance & Control Systems   1
5500 Canoga Ave
Woodland Hills, CA   91364
ATTN: Robert A. Westerholm, Mail Station 87

Officer in Charge of Construction   1
Civil Engineering Laboratory
Naval Facility Engineering Command Detachment
Naval Construction Battalion Center
Port Hueneme, CA   93043
ATTN: Stan Black, Code L40

FMC Corporation   1
Bearing Division
7601 Rockville DR, Box 85
Indianopolis, IN
Attention: E.E. Pfoffenberger
           Manager, Engineering Analysis